Application of Successive Cavity Expansion Theory to Piezocone Tests.

피에조콘 관입 시험에 대한 연속 공동확장이론모델의 적용

Beyong-Seock Lim[1], 임병석, In-Mo Lee[2], 이인모

[1] Senior Researcher, Research Center for Disaster Prevention Science & Technology, Korea University., 고려대학교 방재과학 기술센터, 선임연구원

[2] Professor, Dept. of Civil & Environmental Engineering, Korea University., 고려대학교 토목환경공학과 교수

개   요 : 본 연구는 피에조콘(Piezocone) 관입 시험에 의한 과잉간극수압의 소산 (Dissipation)특성을 파악하기위하여, 실측된 소산실험 결과치와 Gupta & Davidson에 의해 개발된 연속 공동확장이론(Successive Cavity Expansion Theory) 모델을 비교 하였고, 그 경험적 이론의 적합성을 규명하였다. 연속 공동확장 이론이란, 콘 관입이 유발하는 관입 주 변지반의 변환 메커니즘을 연속적인 공동확장의 전개과정로 파악할 때, 관입주변의 연속적 공동확장 영역에서 발생된 과잉간극수압들은 연속적으로 소산되어지고, 결국에는 관입멈춤 직후 얻게되는 소산시험의 결과도 이러한 과잉간극수압의 연속적 소산 메커니즘으로부터 그 영향을 받는다는 개념이다. 본 연구의 실험방법은 Piezocone 관입을 위한 연약모형지반 조 성을 위하여 초대형 Slurry Consolidometer에 Slurry를 45일간 압밀시킨후 Calibration Chamber(Louisiana State University Calibration Chamber System)에 옮긴후 2차 압밀시키 는 Two-Stage Consolidation Method를 사용하였다. 또한, 모형지반내에 8개의 Piezometers 를 설치하여 Piezocone 관입시 유발되는 지반 내에서의 과잉간극수압의 변환을 측정하였다. 실험결과와 이론 예측치를 비교함으로써 연속 공동확장이론 모델은 u_2 형식의 피에조콘 관 입 소산시험 결과들과 잘 들어맞는 모습을 보여줬으나, 관입으로 인한 주변 지반의 과잉간 극수압의 소산변화는 정성적으로만 모사 되는 모습을 보여줬다.

KeyWords : Piezocone, Dissipation Test, Cavity Expenasion Theory, Calibration Chamber, Excess Pore pressure.

1. INTRODUCTION

Determination of the initial excess pore pressure distribution for a accurate dissipation analysis should take into account the dissipation which has already occured during piezocone penetration. The method proposed by Gupta and Davidson (1986), simulating the piezocone penetration process as successive spherical cavity expansions and taking into account the dissipation effect gave very good agreement with the dissipation results at the cone base. The predicted spatial pore pressure distribution during the dissipation phase showed only a qualitative agreement with the experimental results due to the

limitations and simplifying assumptions in the method.

2. BACKGROUND

The pore pressure measured by piezocone can be divided into two components:
- in situ hydrostatic pressure (u_0)
- excess pore pressure generated by piezocone intrusion (Δu)

The excess pore pressure(Δu) is a combination of two different stresses :
octahedral excess pore pressure (Δu_{oct}) and shear induced excess pore pressure (Δu_{shear}), such that

$$\Delta u = \Delta u_{oct} + \Delta u_{shear}$$

Many investigators have proposed various interpretation methods for analyzing the consolidation that occurs when piezocone penetration is stopped. Among them the cavity expansion theory is based on the assumption of undrained soil response and disregarding the shear induced excess pore pressure. The general form of expansion of cavity induced penetration may be visualized from Figure 2.1. The equation of equilibrium in the radial direction is given by:

$$\frac{\partial \sigma_r}{\partial r} + \beta \frac{\sigma_r - \sigma_\theta}{r} = 0$$

where $\beta = 2$ for spherical expansion, $\beta = 1$ for cylindrical expansion. Theories for cylindrical and spherical cavity expansion in soils have been developed by Soderberg(1962), Ladanyi(1963), and Vesic(1972). Torstensson (1977) assumes isotropic initial stress distribution, ideal elastic-perfectly plastic material, undrained one-dimensional cavity expansion and uses a linear, uncoupled finite difference scheme to analyze the pore pressure dissipation and consolidation. The radius of the plastic zone (r_p) is given by:

Cylindrical Cavity Spherical Cavity

$$r_p = r_0 \sqrt{\frac{G}{S_u}} \qquad\qquad r_p = r_0 \sqrt[3]{\frac{G}{S_u}}$$

where r_0 = equivalent penetrometer radius, and G/S_u = I_r = rigidity index. The initial excess pore pressure distribution at any radius r in the plastic zone is given by

Cylindrical cavity $\qquad \Delta u = S_u \left[\ln \frac{G}{S_u} - 2 \ln \frac{r}{r_0} \right]$

Spherical cavity $\qquad \Delta u = 4 S_u \left[\frac{1}{3} \ln \frac{G}{S_u} - \ln \frac{r}{r_0} \right]$

The method suggested by Gupta and Davidson(1986) for simulating the piezocone penetration consists of matching the field piezocone dissipation curve with

computer-generated dissipation plots. The computer plots were obtained by a two dimensional uncoupled axisymmetric dissipation of an assumed initial excess pore pressure distribution. The method assumes that the advance of the cone produces in its immediate vicinity a series of successive spherical cavity expansions (Figure 2.2). Computations are made in an incremental manner to permit pore pressure dissipation during the advance of the probe. Two-dimensional axisymmetric consolidation problem was solved with assumed values of in situ coefficient of consolidation until a good match between the field and computer generated dissipation curves were obtained.
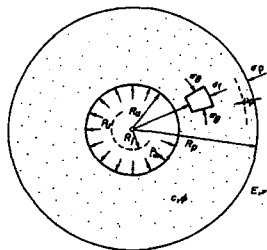

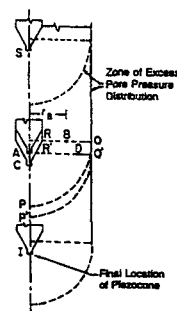Figure 2.1 Expansion of Spherical Cavity (Vesic, 1972)

Figure 2.2 Modeling Piezocone Penetration as Successive Spherical Cavity Expansion (Gupta & Davidson, 1986)

3. TESTS

In this study, miniature piezocone penetration tests and reference piezocone tests were conducted in calibration chamber (LSU/CALCHAS). Dissipation tests were performed at the end of all piezocone penetration tests. Two main phases are used in the test procedure. They are the specimen preparation phase and the penetration phase. The stage of specimen preparation consists of two steps: slurry consolidation in consolidometer, reconsolidation in calibration chamber. Each procedure is involved with heavy instrumentation which provide detailed monitoring of the specimen environment.

Soil slurry(K-33 specimen) was prepared by mixture of 33 % kaolin, 67 % Edgar fine sand and de-aired water by weight. The grain size distribution of the kaolin, fine sand and soil mixture(K-33 specimen) is shown in Figure 3.1. The Atterberg limits of the virgin kaolin, fine sand and K-33 mixture are shown in Table 3.1.

Five specimen were prepared by the technique descrived above. Summary of the stress history of the each specimen and reference soil parameters are shown in Table 3.2 and Table 3.3. All tests were conducted at the standard penetration rate of 20 mm/sec. The general view of data acquisition system set up for calibration chamber test is shown in Figure 3.2. Two kinds of miniature piezocones were utilized for this research (Figure 3.3).

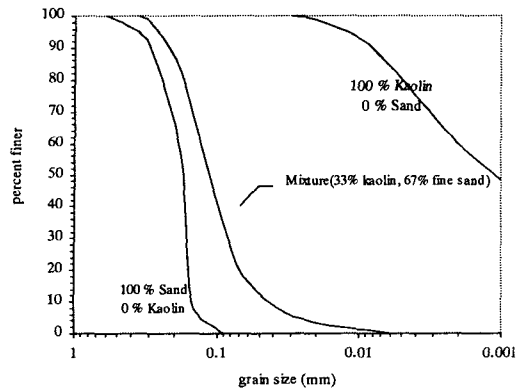## 4. COMPARISON EXPERIMENTAL AND PREDICTED OF INITIAL EXCESS PORE PRESSURE DISTRIBUTION

Figure 3.1 Particle size distribution curves

Soil	Liquid Limit (%)	Plastic Limit (%)	Plasticity Index (%)	Specific Gravity (G)
Kaolinite	54	28	26	2.66
Fine Sand	....	....	....	2.67
Kaolinite and Sand (K33)	20	14	6	....

Table 3.1 Properties of Kaolin and K-33 mixture

Specimen No.	Chamber Consolidation	OCR	Final Effective Stresses (Kpa) Vertical	Horizontal	Lateral Stress Coefficient (K₀)
1	Isotropic	1	207	207	1
2	Anisotropic (K₀)	1	207	86.2	0.42
3	Isotropic	1	262.2	262.2	1
4	Anisotropic (K₀)	1	262.2	104.8	0.40
5	Anisotropic (K₀)	10.9	24.2	40.71	1.70

Table 3.2 Summary of the stress history of the chamber specimens

Specimen No.	Water Content (%)	Undrained Shear Strength S_u (Kpa)	Skempton pore pressure parameter at failure, A_f	Rigidity Index $I_r = G_u/S_u$	Radial Coefficient of Consolidation (c_r x 10⁻³ cm²/sec)
1	17.36	80	0.49	100	1.9
2	19.43	85	0.37	333	4.2
3	17.22	98	0.71	167	2.2
4	17.54	121	0.25	400	4.2
5	16.80	35	-0.02	500	1.8

Table 3.3 Reference soil parameters

Vesic (1972) developed the following expression for consideration of the induced shear pore pressure of the spherical cavity expansion in the analysis of penetration excess pore pressure by introducing the Henkel pore pressure parameter α_f.
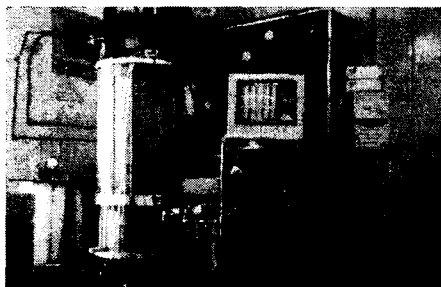

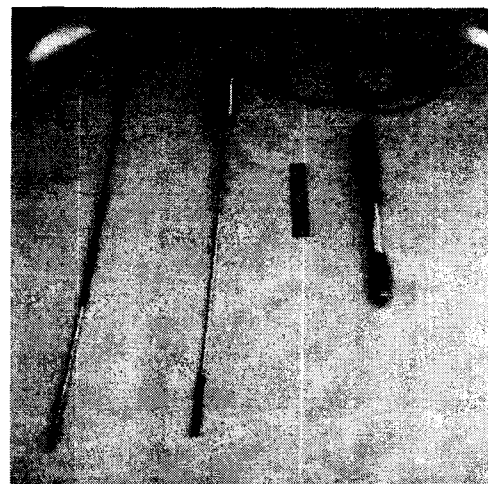Figure 3.2 General view of data acquisition system set up

Figure 3.3 Cone Penetrometers

$$\Delta u = s_u \left[0.943\alpha_f + 4\ln\left(\frac{r_p}{r}\right) \right] \tag{4.1}$$

where s_u, r_p, r are as defined earlier. α_f is related to the Skemptons pore pressure parameter at failure, A_f, by $\alpha_f = 0.707\ (3\ A_f - 1)$.

It was found that the pore pressures predicted by the above equations were still different from the excess pore pressures measured by the piezocone. A correction procedure was hence adopted (proposed by Gupta and Davidson, 1986) for by adjusting equation 4.1 to relate to the measured excess pore pressures. The following expression was used to obtain the corrected initial excess pore pressure distribution:

$$\Delta u_{rc} = \frac{\Delta u_b \left[0.943\alpha_f + 4\ln\left(\frac{r_p}{r}\right) \right]}{\left[0.943\alpha_f + 4\ln\left(\frac{r_p}{r_0}\right) \right]} \tag{4.2}$$

where u_{rc} is the corrected spatial excess pore pressure distribution, and u_b is the actual measured excess pore pressure at the base of the piezocone (i.e. u_2 configuration). The method proposed by Gupta and Davidson (1986) for determining the initial excess pore pressure distribution by successive spherical cavity expansions was used to simulate the piezocone penetration mechanism. The continuous pore pressure dissipation along the penetration path that takes place during the piezocone penetration test was also taken into account. This initial pore pressure distribution was allowed to dissipate during the consolidation phase.

4.1 DISSSIPATION PHASE

The corrected pore pressure distribution was used in a dissipation analysis based on the Terzaghi-Rendulic uncoupled consolidation theory. This theory involves the assumption that the total stress remains constant during the consolidation process. For an axisymmetric linear uncoupled consolidation problem, the governing differential equation is

$$c_r \frac{\partial^2 \Delta u}{\partial r^2} + \frac{c_r}{r}\frac{\partial \Delta u}{\partial r} + c_r \frac{\partial^2 \Delta u}{\partial Z^2} = \frac{\partial \Delta u}{\partial t} \tag{4.3}$$

where r is the radial distance from the axis of the cone. The Crank-Nicolson (Gupta, 1983) scheme to the governing differential equation is given as

$$\frac{1}{2}c_r\delta_r^2\left(\Delta u_{i,j}^{n+1} + \Delta u_{i,j}^n\right) + \frac{1}{2}\frac{c_r}{r}\delta_r\left(\Delta u_{i,j}^{n+1} + \Delta u_{i,j}^n\right) +$$

$$\frac{1}{2}c_r\delta_z^2\left(\Delta u_{i,j}^{n+1} + \Delta u_{i,j}^n\right) = \frac{\left(\Delta u_{i,j}^{n+1} - \Delta u_{i,j}^n\right)}{\Delta t} \tag{4.4}$$

where δ is the central difference operator for the variables. The solution of these equations (locally second-order correct in space and time and unconditionally stable) is

obtained by the Thomas algorithm (Ames, 1977) and is incorporated in program PIEZ (Gupta, 1983). The finite difference mesh used for the analysis is shown in Figure 4.1.
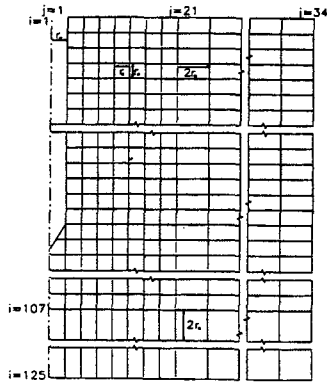
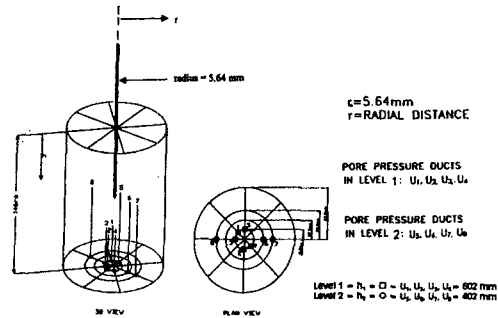

Figure 4.1 Finite Different Mesh

Figure 4.2 Location of pore pressure ducts in the chamber specimen

In the calibration chamber tests conducted, the spatial pore pressure distribution was measured by pore pressure access ducts extending through the aluminum base plate into the specimen. They were installed at two different elevations and at various radial distances from the axis of penetration (Figure 4.2). Since the method proposed by Gupta and Davidson (1986) has a limitation in simulating the tip geometry of piezocone (i.e. u_1 type piezocone penetration), predictions of dissipation curves from specimen 1 which had only u_1 type piezocone penetrations were not shown in Table 4.1.

Comparisons of the predicted dissipation with the dissipation curves monitored at the cone base for the reference cone and the miniature piezocones for the specimens (No. 2 and 5) are shown in Figures 4.3a through 4.3b. Comparisons with the spatial pore

Level of Ducts		Specimen 2 (r/r$_0$)		Specimen 3 (r/r$_0$)	Specimen 4 (r/r$_0$)			Specimen 5 (r/r$_0$)	
		2$_{1/A}$F2O4	2$_{1/A1}$F2O3	3$_{1A}$F2N1	4$_{1/A}$F2N0	4$_{1/A1}$F2N2	4$_{1/A}$F2O4	5$_{1/A}$F2N1	5$_{1/A}$F2O4
Level 1	U1	16.7	32.8	23.9	4.4	31.7	16.7	23.9	16.7
	U2	8.9	25.4	31.7	4.4	34.6	8.86	31.7	8.86
	U3	16.0	35.3	23.0	8.9	38.1	16.0	23.0	16.0
	U4	9.4	19.5	37.2	8.9	32.6	9.4	37.2	9.40
Level 2	U5	22.2	33.9	24.8	8.9	26.6	22.2	24.8	22.2
	U6	22.2	16.3	44.3	17.7	21.1	22.2	44.3	22.2
	U7	29.8	15.0	52.8	26.6	20.2	29.8	52.8	29.8
	U8	29.8	51.6	15.2	26.6	54.4	29.8	15.2	29.8

Table 4.1 Location of Pore Pressure Access ducts in the calibration chamber specimen

pressure dissipation curves for the specimens are shown in Figures 4.4a through 4.4b. The spatial pore pressure dissipation curves (at different radial distances from the axis of penetration) obtained in the present study showed an initial increase in the pore pressure values followed by a decrease (dissipation) at greater time. The pore pressure ducts located closer to the piezocone reached a peak earlier compared to those monitored away from the piezocone. In fact, some of the pore pressures monitored by ducts located far away from the piezocone were increasing even at 10000 seconds. These observations clearly indicate that dissipation occurs primarily in the radial direction. The figures show the time variation of the spatial pore pressure dissipation

results at level 1 (depth of 602 mm) and at level 2 (depth 402 mm). These reading were obtained with the penetration of piezocone being stopped at level 1 (depth of 602 mm).
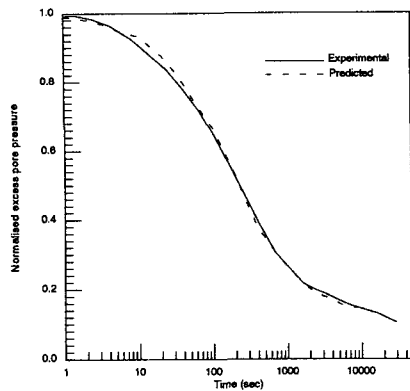

Figure 4.3a Measured and Predicted Dissipation Profiles at the cone base for $4_3/_AF2O4$
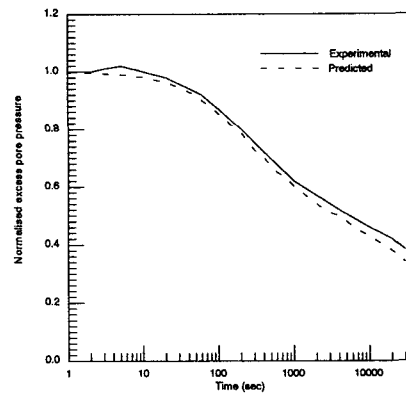

Figure 4.3b Measured and Predicted Dissipation Profiles at the cone base for $5_3/_AF2N1$
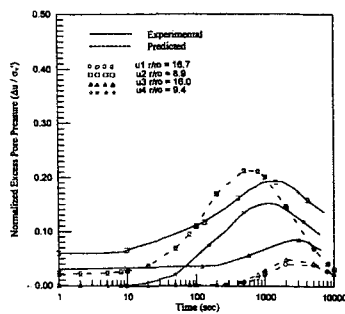

Figure 4.4a Spatial pore pressure dissipation at level 1 in specimen 4 for the dissipation test of $4_3/_AF2O4$ in level 1
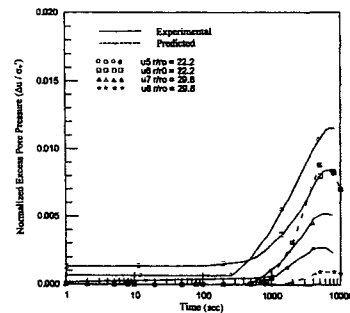

Figure 4.4b Spatial pore pressure dissipation at level 2 in specimen 4 for the dissipation test of $4_3/_AF2O4$ in level 1

The pore pressures predicted by the theory underestimates most of the measured values except reference cone. This could probably mean that the pore pressures below the tip extends to a distance greater than that predicted by spherical cavity expansion and in fact, the pore pressure distribution around the cone tip may not even be spherical in shape.

4.2. DISCUSSION

It can be seen that the dissipation curves predicted at the cone base match very well (Figures 4.3a through 4.3b) with those obtained during the dissipation tests conducted in the specimens. However, the predicted spatial pore pressure dissipation curves (around the piezocone) do not show an accurate match with those of the experiment. The comparisons between the predicted and the measured spatial pore pressure dissipation curves, however, exhibit a fairly good trend agreement considering the limitations and the many simplifying assumptions in the modified cavity expansion

approach. The tip geometry which has a significant influence on the pore pressure gradient around the tip cannot be modeled by a simple method based on a spherical cavity expansion theory. In heavily overconsolidated stiff clays, very high pore pressure gradients develop around the cone tip. The predicted curve of $5_{3/A}$F2N1 (Figure 4.3b) could not simulate the initial increasing part of the dissipation curve. The method proposed by Gupta and Davidson (1986) may not be applied for such soils because it is incapable of predicting such pore pressure gradients which produce a non-standard dissipation curve. It does, however, predict a pore pressure gradient along the length of the penetrometer due to the dissipation effect during penetration. In addition to the above limitations, the model does not take into account the following important factors: geometric nonlinearity due to finite strain rates in the soil during penetration, stress and fabric anisotropy, remolded zone of soil around the penetrometer, coupling between the total stresses and pore pressures, inertia and creep effects.

5. CONCLUSION

The method proposed by Gupta and Davidson (1986) simulates the piezocone penetration process as a successive spherical cavity expansion, and thereby extends the one-dimensional solution proposed by Torstensson to a two-dimensional, axisymmetric problem. The method also takes into account the dissipation that occurs during penetration, and empirically corrects the predicted excess pore pressure at the cone base to exactly match with the measured excess pore pressures. Due to this empirical correction, the method gives very good comparisons between the predicted and actual dissipation profiles above the cone base. However the predicted spatial pore pressure distribution during the dissipation phase show only qualitatively agreement with the experimental results (recorded at the ducts situated along the penetration path). This is probably due to the limitations and simplifying assumptions in the method, because of which the predicted initial spatial excess pore pressures do not exactly match with the actual initial spatial excess pore pressure distribution.

6. REFERENCES

1. de Lima, D. C., 1990, "Development, Fabrication and Verification of the LSU In Situ Testing Calibration Chamber," Ph.D. Dissertation, Louisiana State University, Baton Rouge, LA, 340 p.
2. Gupta, R. C., 1983, "Determination of the Insitu Coefficients of Consolidation and Permeability of Submerged Soils using Electrical Piezoprobe Soundings," Ph.D. Dissertation, University of Florida, 303 p.
3. Gupta, R. C. and Davidson, J. L., 1986, "Piezoprobe Determined Coefficient of Consolidation," Soils and Foundation, Vol. 26, No. 3, pp. 12-22.
4. Kurup, P. U. And Tumay, M. T. Piezocone Dissipation Curves with Initial Excess Pore Pressure Variation, Proceedings, International Symposium on Cone Penetration Testing, CPT95, Linkoping, Sweden, October 1995, pp. 195-200.